PAPER

Synthetic analogues of anthocyanins as sensitizers for dye-sensitized solar cells†

Giuseppe Calogero,*[a] Alessandro Sinopoli,[a,c] Ilaria Citro,[a] Gaetano Di Marco,[a] Vesselin Petrov,[b] Ana M. Diniz,[b] A. Jorge Parola[b] and Fernando Pina*[b]

Seven flavylium salt dyes were employed for the first time as sensitizers for dye-sensitized solar cells (DSSCs). The theoretical and experimental wavelengths of the maximum absorbances, the HOMO and LUMO energy levels, the coefficients, the oscillator strengths and the dipole moments are calculated for these synthetic dyes. The introduction of a donor group in the flavylium molecular structure was investigated. Photophysical and photoelectrochemical measurements showed that some of these synthetic analogues of anthocyanins are very promising for DSSC applications. The best performance was obtained by a DSSC based on the novel compound 7-(*N*,*N*-diethylamino)-3',4'-dihydroxyflavylium which produced a 2.15% solar energy-to-electricity conversion efficiency, under AM 1.5 irradiation (100 mW cm^{-2}) with a short-circuit current density (J_{sc}) of 12.0 mA cm^{-2}, a fill factor of 0.5 and an open-circuit voltage (V_{oc}) of 0.355 V; its incident photocurrent efficiency of 51% at the peak of the visible absorption band of the dye is remarkable. Our results demonstrated that the substitution of a hydroxylic group with a diethylamine unit in position 7 of ring A of the flavylium backbone expanded the π-conjugation in the dye and thus resulted in a higher absorption in the visible region and is advantageous for effective electron injection from the dye into the conduction band of TiO$_2$.

Introduction

Since their appearance in the late eighties,[1,2] nanocrystalline dye-sensitized solar cells (DSSCs)[3] have drawn a lot of attention from the scientific community due to their ease of fabrication, low cost and competitiveness with different photovoltaic systems based on p–n junctions. DSSCs perform also relatively better compared with other solar cell technologies under diffuse light conditions and at higher temperatures. With the development of nanomaterials and molecular design, DSSCs recording efficiencies of up to 13% for small cells[4–8] have been accomplished. The prospect of low-cost investment and fabrication are key features.

DSSCs offer the possibility to design solar cells with a large flexibility in shape, colour, and transparency. Integration into different products opens up new commercial opportunities. In DSSCs, the primary charge separation is achieved by means of a photoexcited dye capable of performing the electron injection into the conduction band of a wide band-gap semiconductor, usually TiO$_2$ (see Fig. 1). Due to its crucial role in such systems, considerable efforts have been directed towards the development and improvement of new families of dyes.
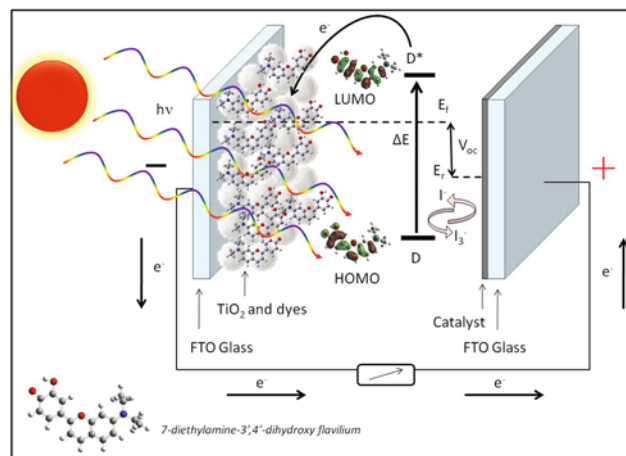

Fig. 1 Schematic representation of the elementary steps involved in a dye-sensitized solar cells based on 7-diethylamine-3',4'-dihydroxyflavylium dye. The frontier orbital plots of HOMO and LUMO were drawn and calculated by Gaussian 09 software.

[a]CNR-IPCF, Istituto per i Processi Chimico-Fisici, via F. Stagno D'Alcontres 37, I-98158 Messina, Italy. E-mail: calogero@me.cnr.it; Fax: +390903974130; Tel: +3909039762247

[b]REQUIMTE, Departamento de Química, Faculdade de Ciências e Tecnologia, Universidade Nova de Lisboa, 2829-516 Caparica, Portugal. E-mail: fp@fct.unl.pt; Fax: +352212948550; Tel: +351212948355

[c]Department of Chemical and Biological Science, University of Huddersfield, Huddersfield, HD1 3DH, UK

†Electronic supplementary information (ESI) available. See DOI: 10.1039/c3pp25347c

The dyes used in DSSC technologies must conform to essential design requirements in order to act as good sensitizers. They must bind strongly to TiO$_2$ by means of an anchoring group, typically carboxylic or hydroxyl groups, to ensure efficient electron injection into the TiO$_2$ conducting band and to prevent gradual leaching by the electrolyte. The dye must absorb solar radiation strongly with absorption bands in the visible or near-IR region, preferably covering a broad range of wavelengths. Electron transfer from the dye to the TiO$_2$ must also be rapid in comparison with decay to the ground state of the dye. The LUMO of the dye must be sufficiently high in energy for efficient charge injection into the TiO$_2$, and the HOMO must be sufficiently low in energy for efficient regeneration of the oxidized dye by the redox couple (Fig. 1). The oxidized and the reduced form of the ground and excited states must be stable.[9]

Usually Ru(II) and Os(II) polypyridine complexes are the most efficient sensitizers in DSSCs. The design and synthesis of polynuclear metal complexes based on luminescent and redox-active building blocks are attractive topics for both theoretical and applicative reasons. In particular, the development of this field would contribute to the design of metal-based supramolecular systems featuring made-to-order energy migration and redox patterns, which could play a role in light-energy conversion. In those systems, the metal-based building blocks were arranged in dinuclear structures by the use of bridging ligands and well-known synthetic strategies.[10–13] These dyes are, however, based on expensive rare metals, require complex multistep syntheses involving toxic and environmentally harmful chemicals which are not sustainable for large mass-scale application. Organic dyes as alternative sensitizers to the Ru(II) complexes exhibit many advantages: (i) the molecular structures of organic dyes are diverse in form and can be easily designed and synthesized; (ii) concerning the cost and environmental issues, organic dyes are superior to noble metal complexes; (iii) the molar extinction coefficients of organic dyes are usually higher than those of Ru(II) complexes, making them attractive for thin film and solid-state DSSCs. However, they also present some disadvantages typical of organic synthetic dyes, mainly the fact that are often less stable than inorganic complexes, need long tedious purification procedures, they are sometimes toxic and their by-products usually are not environmentally friendly. Hagfeldt and co-workers reported a complete description of the most representative synthetic dyes for application in DSSCs.[14]

Recently, natural dyes have shown promise as efficient photosensitizers.[15–17] Several natural dyes are easily available, low in cost, non-toxic, environmentally friendly and fully biodegradable. So, for both practical and fundamental reasons, some groups have investigated the possibility of achieving solar energy conversion exploiting nanocrystalline titania sensitization with natural pigments, mostly from one of the three main families: chlorophylls, betalains and anthocyanins. Of course, for natural sensitizers structural arrangements are not possible, because they developed through Nature's evolution process. In this case the research activity is only limited to select the right natural source for isolation of the identified
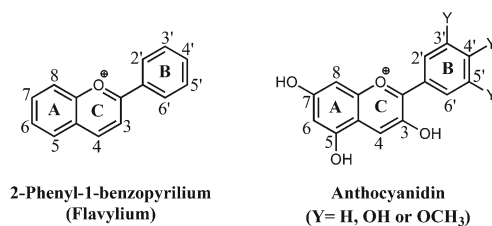

Fig. 2 Chemical structures of 2-phenyl-1-benzopyrylium and anthocyanidins.

sensitizer and find the best operating conditions (concentration, pH, extraction techniques, size of titanium oxide nanoparticles, thickness of photoanode film, soaking time, electrolyte composition, *etc.*).[18–20]

Among natural dyes for DSSCs, anthocyanins are versatile molecules that include the ubiquitous colorants used by Nature to confer colour to most flowers and fruits. They are glycosides of polyhydroxy and polymethoxy derivatives of 2-phenyl-1-benzopyrylium salts (Fig. 2).[21] Anthocyanins occurring in Nature derive from several anthocyanidins or aglycones (Fig. 2), but only six are common in foods – cyanidin, peonidin, pelargonidin, malvidin, delphinidin, and petunidin.[22–24] Research on anthocyanins and related compounds has matured in the last two decades producing many results: discovery and characterization of many new natural compounds,[25–30] clarification of the mechanisms of colour,[31–35] understanding of the kinetic scheme complexity and its exploitation as multistate/multifunctional systems for information processing at the molecular level,[36–38] and for application in solar cells.[16,39] Their colour palette derives in part from their ability to switch between a variety of species (flavylium cations, neutral quinoidal bases, hemiketals and chalcones among others) by means of external stimuli such as pH, temperature and light.

However, for DSSC purposes, it is possible to follow a bio-inspired strategy and with the adequate structural modifications prepare quasi-natural biomimetic compounds. The ideal natural sensitizer could be a dye with similar properties of natural anthocyanins but which could be designed and prepared by simple synthetic procedures, not toxic and environmentally friendly. In the case of the flavylium compounds, progress in the optimization of the design of the sensitizer has been made through the substitution of some groups in the ring or introducing some component in the molecular structure of the dye tailoring desired energy levels and absorption properties.[39]

First of all, we must clarify and stress that the separation between natural anthocyanins and synthetic flavylium salts is rather recent and that from the physical chemistry point of view the two groups are analogous. The chemists who pioneered this field of research did not make such a distinction.[40–44] Synthetic flavylium ions are constituted by the carbon skeleton 2-phenyl-1-benzopyrylium, Fig. 2. The family of compounds exhibiting this basic structure comprises also anthocyanidins, anthocyanins and deoxyanthocyanins that generically belong to the flavonoid class of natural
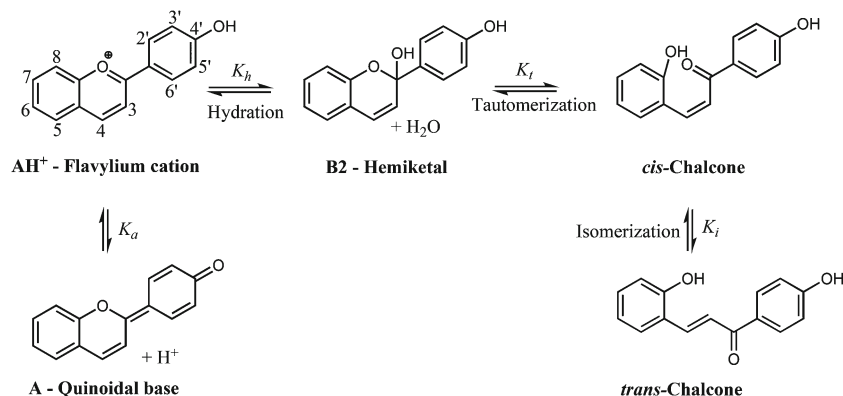
Scheme 1 Flavylium network of chemical reactions.

compounds. It is well known that almost all flavylium compounds, independently of being natural or synthetic, follow the chemical reaction network shown in Scheme 1. The flavylium cation AH[+] is the predominant species in the equilibrium under sufficiently acidic conditions. When the pH is raised the flavylium cation is involved in two parallel reactions: deprotonation to form the quinoidal base A and hydration in position 2 followed by proton loss to give hemiketal B. The *cis*-chalcone Cc is formed from B by a tautomeric process and the *trans*-chalcone Ct forms *via* isomerisation of the former. Depending of the substituents, the pH-dependent mole fraction distribution in the equilibrium (thermodynamic) and the rates of the conversion between different species (kinetic) in the network are different. Distinct photochemistry and photophysical behaviour is also observed depending on the substitution pattern. Usually the photochemically and pH-induced transformations of the flavylium cation are the basis of the design of write-lock-read-unlock-erase cycles for optical molecular level memory with multiple readout capacity.[39] In this work we prepared several flavylium compounds suitable to be employed for the first time as sensitizers in the DSSC technologies. Changing the position and the nature of the substituents in the 2-phenyl-1-benzopyrylium skeleton, a family of seven selected flavylium compounds was synthesized and investigated (Fig. 3). Here we present a complete study of these promising synthetic sensitizers analogous of anthocyanins. For the novel 7-(*N,N*-diethylamino)-3′,4′-dihydroxyflavylium, which presented the best results in DSSCs, a detailed
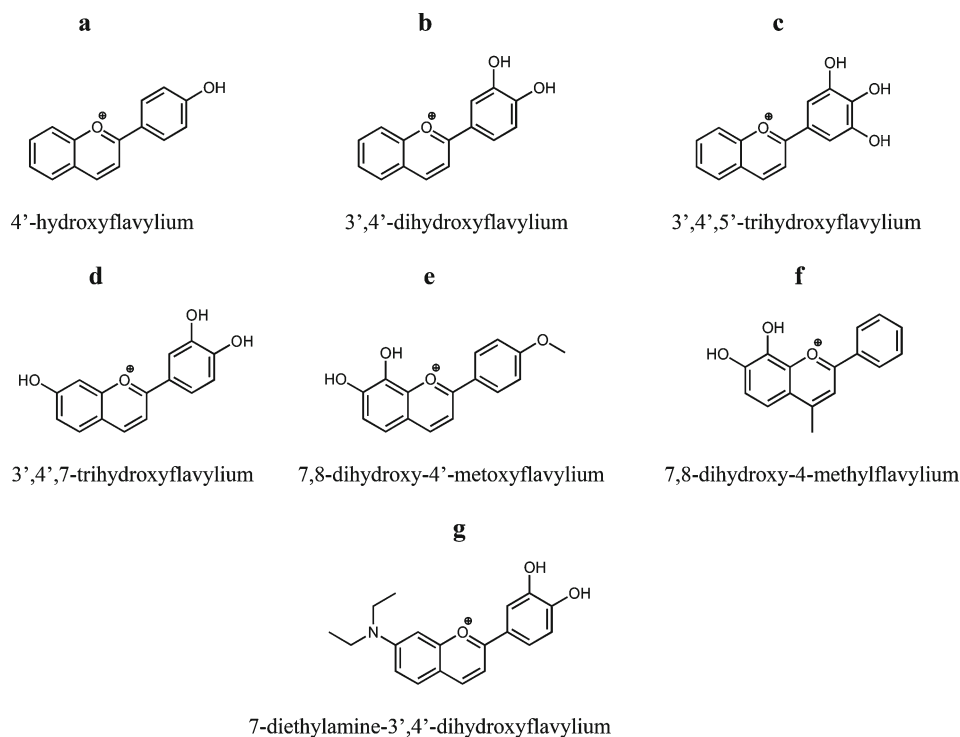

Fig. 3 Chemical structures of the seven flavylium investigated ions.

thermodynamic and kinetic study is also reported aiming to understand how to prepare other flavylium compounds with improved photovoltaic performance of this family of dyes. The new era of "biomimetic" environmentally friendly sensitizers is open.

Experimental

General information and instruments

All solvents and chemicals employed for synthesis and for preparation of samples were of reagent or spectrophotometric grade and were used as received. The absorption spectra of the photo-electrodes were recorded by a Perkin Elmer L20 spectrophotometer UV-Vis (range 180 nm–1100 nm). Current–voltage curves were recorded by a digital Keithley 236 multimeter connected to a PC and controlled by a homemade program. Simulated sunlight irradiation was provided by a LOT-Oriel solar simulator (Model LS0100-1000, 300 W Xe arc lamp powered by LSN251 power supply equipped with AM 1.5 filter, 100 mW cm^{-2}). Incident irradiance was measured with a Si-based pyranometer. Incident photon-to-current conversion efficiency (IPCE) and relative photo-action spectra of sealed DSSCs were measured by a IPCE station. The IPCE station was composed of a 150 xenon light source (model ASB-XE, Spectral Products), a monochromator (model CM110, Spectral Products) equipped with a slit set, a Si calibrated detector (model 818-UV, Newport), a Picoamperometer (model 6487, Keithley) and a IPCE Solarena Software.

NMR spectra were run on a Bruker AMX 400 instrument operating at 400.13 MHz (^{1}H) and 100.00 MHz (^{13}C). UV-Vis spectroscopic experiments were carried out in Millipore water. The pH of the solutions was adjusted by addition of HCl, NaOH or universal buffer of Theorell and Stenhagen,[45] and pH was measured in a Radiometer Copenhagen PHM240 pH/ion meter. UV-Vis absorption spectra were recorded in a Varian-Cary 100 Bio or 5000 spectrophotometer. The stopped flow experiments were conducted in an Applied Photophysics SX20 stopped-flow spectrometer provided with a PDA.1/UV photodiode array detector.

Synthesis

(a) **4′-Hydroxyflavylium hydrogensulfate.** This compound was available from previous studies.[46]

(b) **3′,4′-Dihydroxyflavylium hydrogensulfate.** This compound was prepared from condensation of 2-hydroxybenzaldehyde (4.1 mmol, 0.50 g) and 3′,4′-dihydroxyacetophenone (4.3 mmol, 0.65 g). The reagents were dissolved in 5 ml of acetic acid and 1 ml of 98% H$_2$SO$_4$ was added. The reaction mixture was stirred overnight. By the following day, ethyl acetate was added and a red solid precipitated. The solid was filtered off and carefully washed with ethyl acetate and diethyl ether and dried, yielding 1.21 g of 3′,4′-dihydroxyflavylium hydrogensulfate (3.6 mmol, 88%). ^{1}H NMR (DCl/CD$_3$OD, pD ≈ 1.0, 400.13 MHz) δ (ppm): 9.17 (1H, d, H$_4$, $^3J_{H4–H3}$ = 9.2 Hz), 8.61 (1H, d, H$_3$, $^3J_{H3–H4}$ = 9.2 Hz), 8.22 (4H, m, H$_5$, H$_7$, H$_{5'}$,

H$_{6'}$), 7.99 (1H, d, H$_{2'}$, $^4J_{H2'–H6'}$ = 2.3 Hz), 7.89 (1H, t, H$_6$, $^3J_{H6–H5}$, H6–H7 = 8.00 Hz, $^4J_{H6–H8}$ = 1.20 Hz), 7.13 (1H, d, H$_8$, $^3J_{H8–H7}$ = 8.60 Hz). ^{13}C NMR (DCl/CD$_3$OD, pD ≈ 1.0, 100.00 MHz) δ (ppm): 172.26, 159.74, 156.67, 148.83, 139.12, 131.47, 130.61, 129.03, 124.87, 121.46, 119.87, 118.49, 117.20. Elemental analysis calculated for C$_{15}$H$_{12}$O$_7$S: C 53.57; H 3.60; S 9.53%; found: C 52.77; H 3.19; S 9.82%.

(c) **3′,4′,5′-Trihydroxyflavylium chloride.** This compound was prepared from condensation of 2-acetylbenzaldehyde[47] (2 mmol, 0.32 g) and 2′,3′,4′-trihydroxyacetophenone (12 mmol, 2.01 g). 2′,3′,4′-Trihydroxyacetophenone was dissolved in 98 ml of MeOH. The solution was saturated with dry hydrogen chloride.[48] Upon a *ca.* 15% increase in the volume, the HCl bubbling was stopped and 2-acetylbenzaldehyde previously dissolved in 35 ml of MeOH was added to the mixture at 0 °C and left at room temperature overnight. The solution was concentrated and a solid precipitated out upon addition of diethyl ether. The solid was filtered off, carefully washed with diethyl ether and vacuum-dried. Recrystallization from HCl/MeOH yielded 0.27 g (0.92 mmol, 46%) of 3′,4′,5′-trihydroxyflavylium chloride. ^{1}H NMR (DCl/CD$_3$OD, pD ≈ 1.0, 400.13 MHz) δ (ppm): 9.03 (1H, d, H$_4$, $^3J_{H4–H3}$ = 9.4 Hz), 8.93 (1H, d, H$_3$, $^3J_{H3–H4}$ = 9.4 Hz), 8.15 (3H, m, H$_5$, H$_6$, H$_8$), 7.94 (1H, d, H$_5$, $^3J_{H5–H6}$ = 9.3 Hz), 7.82 (1H, m, H$_7$), 6.74 (1H, d, H$_6$, $^3J_{H6–H5}$ = 9.3 Hz). (DCl/CD$_3$OD, pD ≈ 1.0, 400.13 MHz) d (ppm): 9.03 (1H, d, H$_4$, $^3J_{H4–H3}$ = 9.4 Hz), 8.93 (1H, d, H$_3$, $^3J_{H3–H4}$ = 9.4 Hz), 8.15 (3H, m, H$_{2'}$, H$_{6'}$, H$_8$), 7.94 (1H, d, H$_5$, $^3J_{H5–H6}$ = 9.3 Hz), 7.82 (1H, m, H$_7$), 6.74 (1H, d, H$_6$, $^3J_{H6–H5}$ = 9.3 Hz). ^{13}C NMR (DCl/CD$_3$OD, pD ≈ 1.0, 100.00 MHz) d (ppm): 173.27, 157.42, 155.09, 154.20, 151.65, 137.05, 133.30, 129.71, 128.65, 123.90, 122.93, 120.06, 118.18, 111.27, 109.02. Elemental analysis calculated for C$_{15}$H$_{11}$ClO$_4$·1/2H$_2$O: C 60.11; H 4.04%; found: C 60.63; H 3.91%.

(d) **3′,4′,7-Trihydroxyflavylium chloride.** This compound was prepared from condensation of 2,4-dihydroxybenzaldehyde (5 mmol, 0.69 g) and 3′,4′-dihydroxyacetophenone (5 mmol, 0.76 g). The reagents were dissolved in 12 ml of acetic acid and 3 ml of 98% H$_2$SO$_4$. The reaction mixture was stirred overnight. By the following day diethyl ether was added and a orange solid precipitated. The solid was filtered off and carefully washed with diethyl ether and dried, yielding 0.72 g (2.04 mmol, 40%) of 3′,4′,7-trihydroxyflavylium hydrogensulfate. Recrystallization from HCl/MeOH 3′,4′,7-trihydroxyflavylium chloride was obtained: ^{1}H NMR (DCl/CD$_3$OD, pD ≈ 1.0, 400.13 MHz) δ (ppm): 9.03 (1H, d, H$_4$, $^3J_{H4–H3}$ = 8.8 Hz), 8.28 (1H, d, H$_3$, $^3J_{H3–H4}$ = 8.8 Hz), 8.13 (1H, d, H$_5$, $^3J_{H5–H6}$ = 8.9 Hz), 8.01(1H, dd, H$_{6'}$, $^3J_{H6'–H5'}$ = 8.6 Hz, $^4J_{H6'–H2'}$ = 2.2 Hz), 7.86 (1H, d, H$_{2'}$, $^4J_{H2'–H6'}$ = 2.2 Hz), 7.53 (1H, d, H$_8$, $^4J_{H8–H6}$ = 1.8 Hz), 7.39 (1H, dd, H$_6$, $^3J_{H6–H5}$ = 8.88 Hz, $^4J_{H6–H8}$ = 1.8 Hz), 7.08 (1H, d, H$_{5'}$, $^3J_{H5'–H6'}$ = 8.6 Hz). ^{13}C NMR (DCl/CD$_3$OD, pD ≈ 1.0, 100.00 MHz) δ (ppm): 172.26, 168.48, 158.62, 155.86, 152.47, 146.97, 132.39, 125.00, 120.75, 120.25, 118.43, 116.68, 114.95, 112.27, 102.30. Elemental analysis calculated for C$_{15}$H$_{11}$ClO$_4$·H$_2$O: C 58.36; H 4.24%; found: C 58.56; H 4.04%.

(e) **7,8-Dihydroxy-4′-methoxyflavylium chloride.** This compound was prepared from condensation of 2,3,4-

886 | *Photochem. Photobiol. Sci.,* 2013, **12**, 883–894

This journal is © The Royal Society of Chemistry and Owner Societies 2013

trihydroxybenzaldehyde (3 mmol, 0.46 g) and 4′-methoxyaceto-phenone (3 mmol, 0.45 g). The reagents were dissolved in 9 ml of acetic acid and 2 ml of 98% H_2SO_4. The reaction mixture was stirred overnight. The following day diethyl ether was added and a dark maroon solid precipitated. The solid was filtered off and carefully washed with diethyl ether and dried yielding 0.80 g (2.2 mmol, 76%) of 7,8-dihydroxy-4′-methoxy-flavylium hydrogensulfate. From recrystallization in HCl/MeOH 7,8-dihydroxy-4′-methoxyflavylium chloride was obtained (0.45 g, 49%): ^{1}H NMR (DCl/CD_3OD, pD ≈ 1.0, 400.13 MHz) δ (ppm): 9.05 (1H, d, H_4, $^3J_{H4\ H3}$ = 8.8 Hz), 8.48 (2H, d, $H_{2'}$, $H_{6'}$, $^3J_{H2'6'-H2'6'}$ = 9.0 Hz), 8.29 (1H, d, H_3, $^3J_{H3-H4}$ = 8.8 Hz), 7.67 (1H, d, H_6, $^3J_{H6-H5}$ = 8.8 Hz), 7.41 (1H, d, H_5, $^3J_{H5-H6}$ = 8.8 Hz), 7.20 (2H, d, $H_{3'}$, $H_{5'}$, $^3J_{H3',H5'-H2',6'}$ = 9.0 Hz), 3.92 (3H, s, CH_3). Elemental analysis calculated for $C_{16}H_{13}ClO_4·H_2O$: C 59.54; H 4.68%; found: C 59.29; H 4.03%.

(f) 7,8-Dihydroxy-4-methylflavylium hydrogensulfate. This compound was available from previous studies.[49]

(g) 7-(N,N-Diethylamino)-3′,4′-dihydroxyflavylium chloride. This compound was prepared from condensation of 2-hydroxy-4-diethylaminebenzaldehyde (4 mmol, 0.77 g) and 3′,4′-di-hydroxyacetophenone (4 mmol, 0.61 g). The reagents were dissolved in 12 ml of acetic acid and 3 ml of 98% H_2SO_4. The reaction mixture was stirred overnight. By the following day diethyl ether was added and a dark green solid precipitated. The solid was filtered off and carefully washed with diethyl ether and dried yielding 1.14 g (2.8 mmol, 76%) of 7-(N,N-diethylamino)-3′,4′-dihydroxyflavylium hydrogensulfate. From recrystallization in HCl/MeOH 7-(N,N-diethylamino)-3′,4′-di-hydroxyflavylium chloride was obtained (0.67 g, 48%): ^{1}H NMR (DCl/CD_3OD, pD ≈ 1.0, 400.13 MHz) δ (ppm): 8.57 (1H, d, H_4, $^3J_{H4-H3}$ = 8.2 Hz), 7.90 (1H, d, H_5, $^3J_{H5-H6}$ = 9.3 Hz), 7.78 (2H, d, H_3, $H_{6'}$), 7.70(1H, s, $H_{2'}$), 7.39 (1H, d, H_6, $^3J_{H6-H5}$ = 9.3 Hz), 7.20 (1H, s, H_8), 7.00 (1H, d, $H_{5'}$, $^3J_{H5'-H6'}$ = 8.36 Hz). ^{13}C NMR (DCl/CD_3OD, pD ≈ 1.0, 100.00 MHz) δ (ppm): 167.90, 159.30, 156.30, 153.15, 148.39, 146.44, 132.01, 122.29, 120.92, 117.85, 117.45, 116.18, 114.00, 107.95, 95.67, 45.71 (NCH_2), 11.39 (CH_3). Elemental analysis calculated for $C_{19}H_{20}ClNO_3·H_2O$: C 62.72; H 6.09%; found: C 63.18; H 6.10%.

Computational methods

The initial structures of the compounds were prepared with Gauss View 2.0. The optimization of geometries of the ground state of the seven flavylium dyes was carried out employing density functional theory (DFT) calculations method with B3LYP functional and the basis set 6-31+G(d).[50,51] The theoretical evaluation of the electron density in the HOMO and LUMO of the dye molecules and the vertical electronic excitations were calculated using the time-dependent density functional theory (TDDFT) with B3LYP functional and the same basis set mentioned above.[52] Obtaining accurate UV-Vis spectra from computational methods[53] is not the main aim of this study; therefore the excited states are examined in the solvent-free molecular forms of these natural dyes. The oxidation potentials and the excitation energies for the investigated dyes were determined from TDDFT analysis. The

molecules' ground state geometries, dipole moments and frontier orbital plots of HOMO and LUMO were drawn and calculated by Gaussian 09 software.

Fabrication of DSSCs

The conductive glass plates 2.2 mm thick (FTO glass, fluorine-doped SnO_2, sheet resistance 15 Ω cm^{-2}) and the titanium oxide (TiO_2) paste T/SP (nanoparticles diameter < 25 nm) were purchased from Solaronix SA. The photoanodes were prepared depositing TiO_2 film on the FTO conducting glass plates (sized 1.5 cm × 1.5 cm) by doctor blade: two opposite edges of the FTO glass plate were covered with two stripes of an adhesive tape (3 M Magic) both to control the thickness of the film and to mask electric contact strips. The TiO_2 paste was spread uniformly on the substrate by sliding a glass rod along the tape spacer and then the two adhesive tape stripes were removed. After drying the TiO_2, the anode glass plates were sintered in air for 30 minutes at 450 °C. The resulting mesoscopic oxide film was transparent, with a thickness of about 10 μm. The photoanodes employed for the UV-Vis absorption measurement were made using a screen printer, using a mesh size of 100.40 in polyester fibres in order to obtain a transparent ultra-thin TiO_2 film with an estimated thickness, after sintering process, of about 2 μm. The cooled photoanodes were soaked for 2 h in a 5×10^{-4} M ethanol solution at room temperature in the dark. The excess dye was removed by rinsing with ethanol and then the photoanode was dried in an oven (80 °C) for a short time. The electrolyte solution was optimized for the flavylium salt using 0.05 M I_2 and 0.7 M LiI in acetonitrile. Counter-electrodes were prepared by sputtering a light reflecting Pt mirror (>500 nm thick) onto an FTO conductive glass. The sputtering system consisted in a 150 watt RF-magnetron which generally works at low pressure (10^{-5}–10^{-3} Torr) under a N_2 gas flow.[54] Parafilm® sealed cells (0.25 cm^2 active area) were built by pressing the sensitized photoanode against a platinum-sputtered counter-electrode. The photoanode and the platinum counter-electrode were assembled and clipped in a sandwich-type arrangement with the electrolyte solution placed in between; Parafilm® frame was used to confine the liquid electrolyte inside the cell. The thickness of the liquid layer corresponded roughly to the thickness of the frame borders (~100 μm). In this configuration the solar cell was stable towards solvent evaporation and leaking for several days even when using volatile solvents like acetonitrile.

Result and discussion

Synthetic strategy

The synthesis of flavylium compounds is commonly achieved through the acid-catalyzed condensation of acetophenones with salicylaldehydes (see ESI†), often following a method introduced early by Robinson[48] and slightly modified by Katritzky et al.[55] The flavylium salts used in this study were either available from previous studies (4′-hydroxyflavylium hydrogensulfate[46] and 7,8-dihydroxy-4-methylflavylium

hydrogensulfate[49]) or synthesized following the above procedures. In the case of flavylium compounds with three or more hydroxyl groups, higher yields are usually obtained if the salicylaldehyde is previously acylated; this strategy was used in the synthesis of 3′,4′,7-trihydroxyflavylium chloride.[56]

Optical properties and computational analysis

An important thermodynamic requirement of the dyes to be used in DSSC technology is that the HOMO level of the sensitizer has to be sufficiently positive in the redox potential for efficient regeneration of the oxidized dye molecule to its original state by the iodide electrolyte and the LUMO energy of the dye has to be sufficiently higher than the conduction band edge of the semiconductor (E_{CB}).[57] All the seven studied compounds, in ethanol solution, exhibited a good absorption maximum in the UV-Vis region and this optical property makes them potential candidates for light harvesting in DSSCs (see experimental data in Table 1). In previous work, complexation of flavylium derivatives with Al^{3+} bearing a catechol unit at positions 3′,4′ as well as natural anthocyanidins, cyanin and luteolinidin, was described.[49] The blue color in Nature is obtained by a supramolecular structure involving metal complexation of the *o*-dihydroxy groups in ring B. According to our best knowledge, adsorption of flavylium synthetic dyes to the semiconductor was performed for the first time. This reaction is completed in 120 minutes, as reported in the experimental part. The formation of blue films in the present compounds is an indication of the quinoidal base interaction with TiO_2 and by consequence the DFT and TDDFT calculations were performed considering this species. In fact, all the dyes, when deposited onto TiO_2 film, showed three typical absorption features: a shoulder at *ca.* 380 nm and two bands around 440 and 540 nm (Fig. 4). Compound c showed the most intense absorption band (440 nm). Comparing compound c with compound b the latter presents a broader band shifted to the red by 50 nm, due to the removal of a hydroxylic group. The optimized ground state geometries were used to assess the structural contribution of the molecule to its photophysical properties. All the seven compounds present a planar structure in the quinonoidal form. The theoretical and experimental wavelengths of the maximum absorbance, the HOMO and LUMO energy level, the coefficients, the oscillator strength and the dipole moment are shown in Table 1. The charge
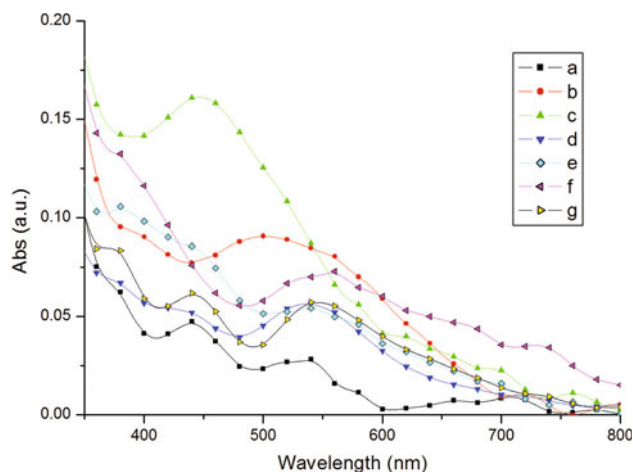

Fig. 4 UV-Vis absorption spectra of flavylium dyes absorbed on a 2 μm thick TiO_2 film screen-printed on FTO glass.

distribution in the frontier molecular orbitals is depicted in Table 2a. In Table 2b are showed the charge distribution in the frontier of molecular orbitals for some of the investigated flavylium dyes (b, d, g). As reported by Cherepy *et al.*,[58] the presence of Ti(IV) shifts the absorption spectra in the red region and consequently changes the charge distribution. From Table 2b for the quinonoidal form complexed with Ti(IV), the HOMO (highest occupied molecular orbital) is more located on the chromophore end of the complex, while the LUMO (lowest unoccupied molecular orbital) electron density is more located near the Ti(IV) end. The calculated excited state energies are all higher than the conduction band edge of the TiO_2, which usually depends on different conditions like the pH (see ref. 16). Scheme 2 depicts the energy-level diagram of the ground state (HOMO) and of the singlet excited state (LUMO) of each flavylium ion in quinoidal form. Increasing the number of the hydroxylic groups in compounds (a), (b) and (c) decreases the LUMO energy state while the HOMO energy increases, reducing the theoretical energy gap (Table 1). The introduction of one or more hydroxylic groups in the ring A of (a) or (b) increases both the HOMO and the LUMO energy levels, as shown for compounds (d) and (e). As suggested from the data reported in Scheme 2, all the flavylium dyes should be capable of injecting electrons into the conducting band of TiO_2 upon excitation; if they are not able, there may be other

Table 1 Calculated (TDDFT/B3LYP) ground state and excitation state, spectral characteristics, configuration coefficient (*C*), oscillator strength (*f*) and dipole moment for flavylium dyes in quinoidal form

	Cation	Energy (eV)		Absorption maximum (eV)		*C*	*f*	Dipole moment (debye)
		HOMO	LUMO	Theoretical	Experimental			
a	4′-Hydroxyflavylium	−5.67758	−2.90586	2.78	3.26	0.56	0.545	10.0059
b	3′,4′-Dihydroxyflavylium	−5.49118	−2.93933	2.60	2.51	0.55	0.515	9.0012
c	3′,4′,5′-Trihydroxyflavylium	−5.45009	−2.9992	2.54	2.62	0.51	0.478	8.00227
d	3′,4′,7-Trihydroxyflavylium	−5.39730	−2.83784	2.64	2.46	0.33	0.615	10.8328
e	7,8-Dihydroxy-4′-methoxyflavylium	−5.32247	−2.78423	2.13	2.56	0.61	0.158	9.6074
f	7,8-Dihydroxy-4-methylflavylium	−5.34887	−2.89498	2.00	2.33	0.61	0.110	8.0211
g	7-Diethylamino-3′,4′-dihydroxyflavylium	−5.07260	−2.5601	2.56	2.18	0.56	0.806	12.2103

Table 2 (a) HOMO and LUMO of the flavylium dyes; (b) HOMO and LUMO of the flavylium dyes attached to Ti(IV)
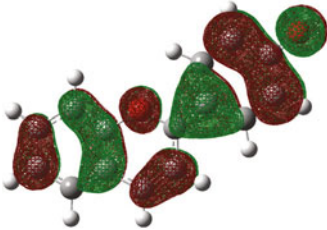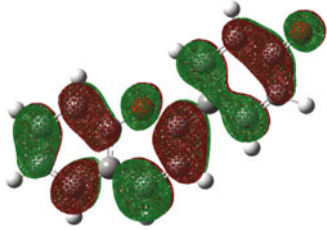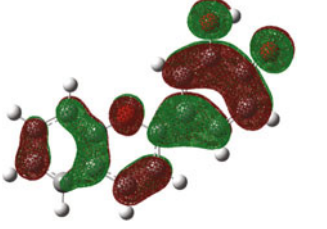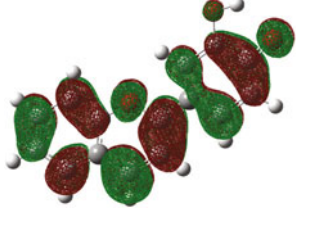
(a)
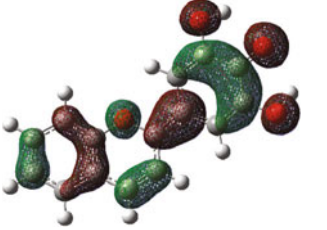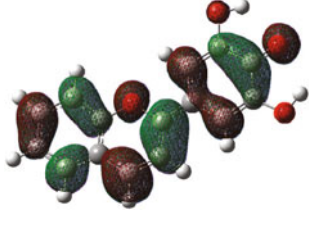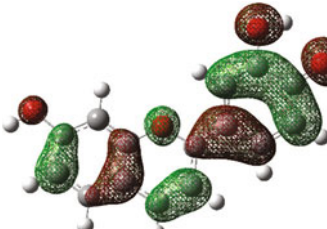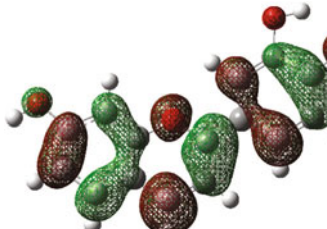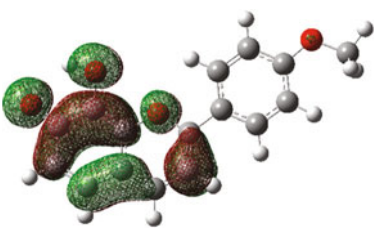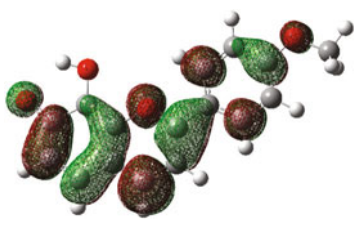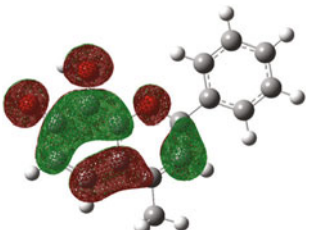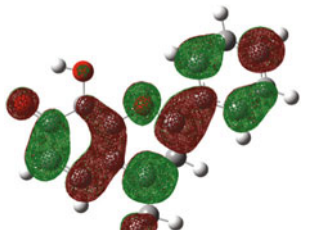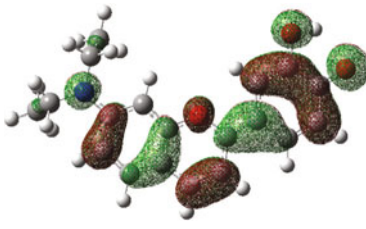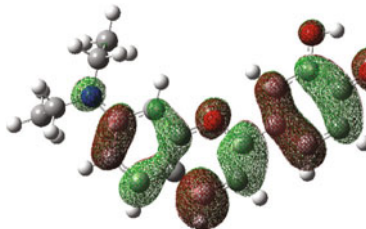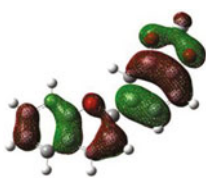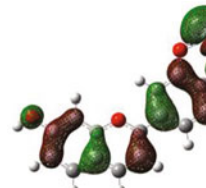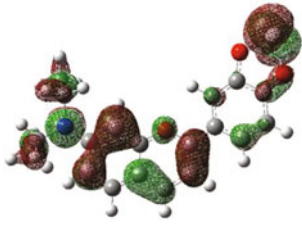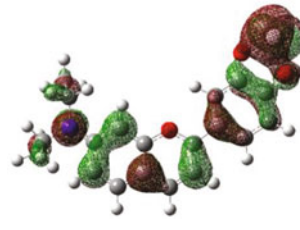
Pigment	HOMO	LUMO
(a) 4′-Hydroxyflavylium		
(b) 3′,4′-Dihydroxyflavylium		
(c) 3′,4′,5′-Trihydroxyflavylium		
(d) 3′,4′,7-Trihydroxyflavylium		
(e) 7,8-Dihydroxy-4′-methoxyflavylium		
(f) 7,8-Dihydroxy-4-methylflavylium		

This journal is © The Royal Society of Chemistry and Owner Societies 2013

Photochem. Photobiol. Sci., 2013, **12**, 883–894 | **889**

Table 2 *(Contd.)*

(a)

Pigment	HOMO	LUMO
(g) 7-Diethylamine-3′,4′-dihydroxyflavylium		

(b)

Pigment	HOMO	LUMO
(b) 3′,4′-Dihydroxyflavylium		
(d) 3′,4′,7-Trihydroxyflavylium		
(g) 7-Diethylamine-3′,4′-dihydroxyflavylium		
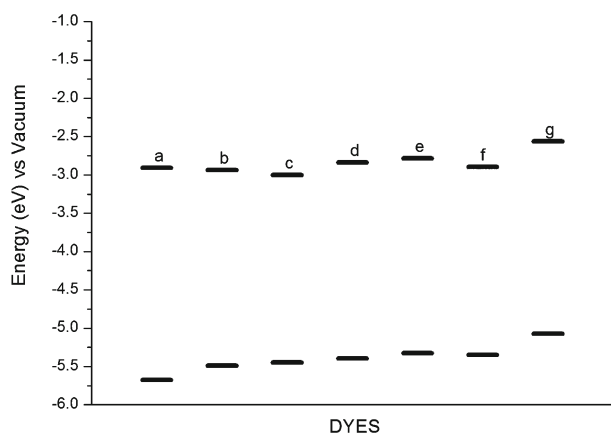
Scheme 2   Energy level diagram of the investigated flavylium dyes.

factors that avoid this deactivation pathway. Furthermore all the flavylium compounds possess a HOMO level energy below the conventional potential of the iodide/triiodide redox couple and this means that the electrolyte is able to reduce the oxidized dye after the injection process into TiO_2. Because the data depicted in Scheme 2 are calculated and are not experimental, we used these data only to estimate the energy level. Detailed characterization of experimental properties and values of HOMO and LUMO of flavylium dyes will be discussed in a future paper. In Fig. 5, the optimized geometries of the ground state of the investigated dyes with the corresponding dipole moment of the quinoidal form are presented. As shown in Fig. 5A, the dipole moment increases by decreasing the number of OH groups in ring B. On the other hand, comparison of compound (b) with compound (d) shows that the introduction of a OH group in position 7 leads to an increase of the dipole moment. Also, substituting the OH group in position 7 by a stronger electron donor such as *N,N*-diethylamine leads to an increase of the dipole moment (Fig. 5B). Comparing compounds (e) and (f) (Fig. 5c), the former presents a higher
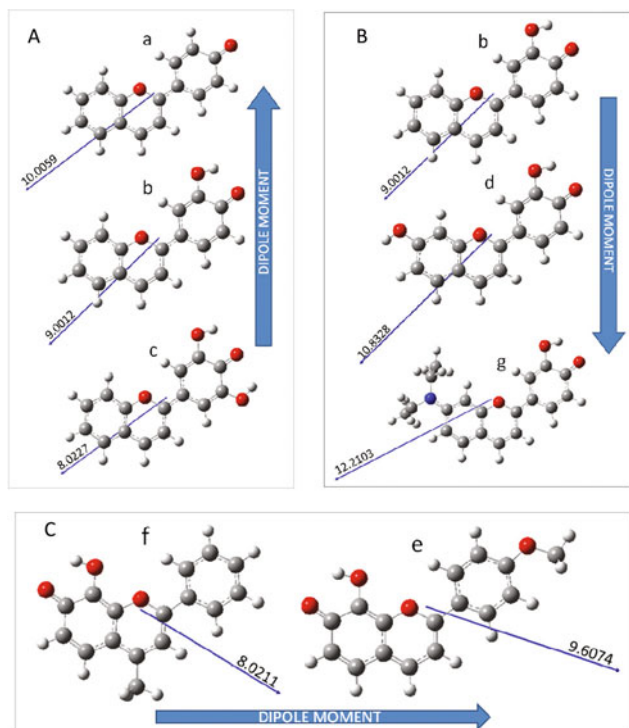
Fig. 5 Optimized ground state geometry and dipole moment calculated by Gaussian 09 software for the seven flavylium dyes.

dipole moment than the latter because of the introduction of a OCH$_3$ group in position 4′ of ring B. In conclusion, the introduction of an electron-rich group (hydroxyl, methoxy, diethylamine, *etc.*) in ring B or in the ring A decreases or increases the dipole moment depending on the orientation of the vector representing the dipole moment: if the electron-rich group is inserted into the less electron-rich part of the molecular structure the dipole moment decreases (Fig. 5a), otherwise it increases (Fig. 5b and 5c). The increment of the dipole moment results in an increase of the sensitizing performance of the dye.

The thermodynamic and kinetic constants of the network of chemical reactions regarding the most promising flavylium compound, 7-(*N,N*-diethylamino)-3′,4′-dihydroxyflavylium, were studied in aqueous solution (see ESI†). The value of pK'_a = 4.8 indicates that the lone pair of the amino group is delocalized into the benzopyrylium ring.[59] In the quinoidal base, a similar delocalization is also present as shown by the red-shifted absorption maximum when compared with flavylium cations bearing only hydroxyl groups.[39] While in water the compound exhibits the general pattern of the family, when linked to the TiO$_2$ semi-conductor the base is stabilized preventing the hydration to give hemiketal and the chalcones. Stabilization of the quinoidal base in the presence of Al^{3+} was previously reported in solution.[49]

Photovoltaic performance of DSSCs

The ground and excited states of the present flavylium dyes exhibit the necessary thermodynamic requirements to be suitable sensitizers for DSSCs, as discussed above. The parameters of DSSCs sensitized with these seven flavylium dyes, *i.e.*, short circuit current density (J_{sc}), open circuit voltage (V_{oc}), fill factor (ff) and the overall conversion efficiency (η), measured under AM 1.5 solar light (100 mW cm^{-2}), are summarized in Table 3 and the photocurrent–voltage (J–V) plots are shown in Fig. 6. The effect of the position of the hydroxylic group on the photoelectrochemical behaviour of the flavylium dyes when applied in the DSSC technologies was studied. Comparing compound (a) with compound (b) we found that the latter exhibits a better J_{sc}, around seven-fold more intense, with a corresponding η fifteen times better; this is related to the greater chelating effect of the catechol group in (b) when compared with the monohydroxylic group in compound (a). With the introduction of a donor group (OH) in ring A of compound (b) we obtained compound (d); the donor ability of the hydroxylic group increases the dipole moment (Fig. 5) and increases both the ground (HOMO) and the excited state (LUMO) energies (Scheme 2). The presence of the hydroxyl group in position 7 of compound (d) enhances the J_{sc} of this compound, and increases its corresponding η up to 1.22%. On introducing a stronger donor group in position 7 such as diethylamine, compound (g) is obtained with observed further

Table 3 Photovoltaic performance of DSSCs based on flavylium dyes

Dye	J_{sc} [mA cm^{-2}]	V_{oc} [mV]	ff	J_{max} [mA cm^{-2}]	V_{max} [mV]	η [%]
a	0.70	140	0.41	0.41	100	0.041
b	5.20	254	0.47	4.35	150	0.63
c	0.46	198	0.50	0.3	150	0.046
d	6.37	342	0.55	5.49	225	1.22
e	1.72	225	0.53	1.38	150	0.208
f	2.50	119	0.39	1.55	75	0.116
g	12.03	355	0.50	9.54	225	2.15
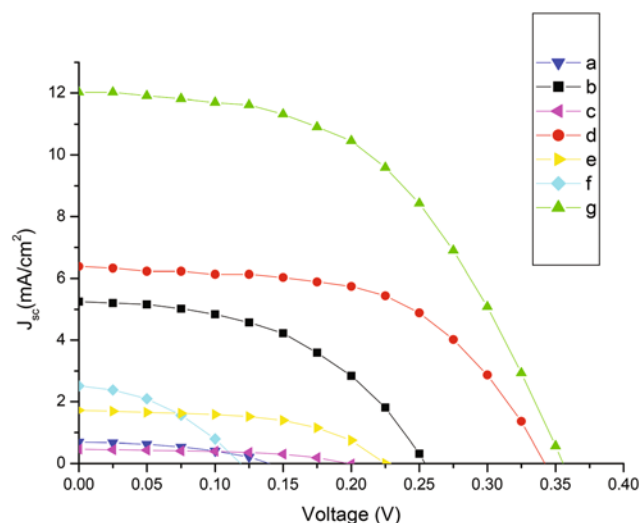
Fig. 6 *J*–*V* curves of DSSCs based on flavylium dyes under 100 mW cm^{-2} simulated AM 1.5 illumination.

This journal is © The Royal Society of Chemistry and Owner Societies 2013

Photochem. Photobiol. Sci., 2013, **12**, 883–894 | **891**

enhancement of the current density up to 12 mA cm^{-2} together with a corresponding photoconversion efficiency of 2.15%, measured under AM 1.5 irradiation. For this compound and for compound (d) the high J_{sc} values contribute to increase the V_{oc} up to 0.355 and 0.342, respectively. In compound (g), the calculated HOMO and LUMO energies are located higher than those of the other flavylium compounds due to the better donor ability of the diethylamine group. Consequently, compound (g) exhibits a higher driving force for electron transfer between the dye and the semiconductor. The replacement of a hydroxyl group with a diethylamine unit in position 7 of the flavylium core expands the π-conjugation in the dye increasing the effective electron injection from the dye into the conduction band of TiO$_2$. The diethylamine donor group acts as an electron donor (D), the catechol moiety in ring B behaves as an acceptor (A) and the benzopyran systems (rings A and C) constitute a π bridge (in the quinoidal form) defining a D–π–A structure. From the comparison of the efficiency between compounds (f) and (b), it is evident that the DSSC efficiency increases when the catechol group is located in ring B because when the catechol is on ring A, on the same side of the HOMO location, there is no good charge separation between the excited electron and the hole (Table 2). For compound (g), the best performance is due to the presence of diethylamine, an electron donor, which can separate the photoinduced electron and hole by donating electrons. This is confirmed from the comparison between compounds (e) and (d), where the latter exhibits a better photoconversion efficiency and produces a higher J_{sc}. Concerning compound (c), it shows an anomalous behaviour with a photovoltaic performance almost the same as compound (a). In this case the introduction of a third hydroxyl group in ring B decreases J_{sc}, showing that the extra OH group affects the neighbour catechol group injection properties. Furthermore, its dipole moment is lower than that of compound (a) and this implies that in the ground state the HOMO of compound (c) is more delocalized in the whole molecular structure than in (a). The IPCE corresponds to the number of electrons, measured as photocurrent in the external circuit, divided by the monochromatic photon flux that strikes the cell. Other names for IPCE include calibrated spectral response and external quantum efficiency (EQE). Concerning the IPCE measurements, the best value (51%) was reached for compound (g) (see Fig. 7) and the photo-action spectra exhibit the same profile as the corresponding absorption spectra of the dye (Fig. 4). It is worth noting how the obtained value is approaching the theoretical limit of 69% predicted by Grätzel and co-workers in 1997 for natural anthocyanins (a mixture of cyanidin-3-glycoside and cyanidin-3-rutinoside).[58]

Conclusions

Seven flavylium salt dyes were employed for the first time as sensitizers for dye-sensitized solar cells (DSSCs). The compound 7-(N,N-diethylamino)-3′,4′-dihydroxyflavylium exhibits
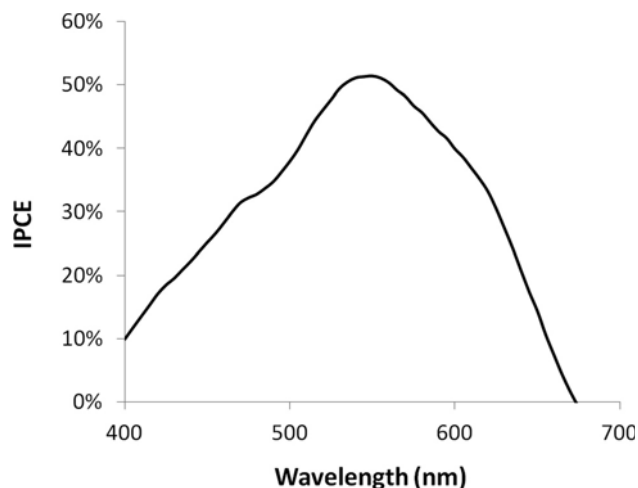

Fig. 7 IPCE spectra for DSSC sensitized by 7-(N,N-diethylamino)-3′,4′-dihydroxyflavylium (compound (g)).

the best photovoltaic performance among the investigated flavylium dyes. A detailed investigation of how the introduction of OH, OCH$_3$ and N(CH$_2$CH$_3$)$_2$ electron-donor groups in the flavylium structure affects the sensitization activity was carried out. The results from DFT and TDDFT computational analysis showed that the largest dipole moments arise when the electron donor groups align with the anchoring catechol moiety, increasing the electron injection into the semiconductor. This effect is larger when the dimethylamino group in position 7 is aligned with the catechol group in positions 3′,4′. The presence of the catechol unit was shown to be essential for anchoring the dye to the Ti(IV) centers of the semiconductor since monohydroxylic flavylium cations showed very low light to electricity conversion efficiency. This implies that natural compounds such as malvidin, peonidin and pelargonidin and their aglycones are not suitable to be employed in DSSC, while cyanidin and its derivatives are very promising. The present study gives for the first time the knowledge to design more efficient flavylium dyes with introduction of donor/acceptor groups in adequate positions of the flavylium skeleton.

In conclusion, it is possible to follow a bio-inspired strategy and with the adequate structural modifications prepare quasi-natural biomimetic, non-toxic and environmentally friendly compounds by simple synthetic procedures suitable to be employed in DSSC technologies. The new era of "biomimetic" environmentally friendly sensitizers is open.

Acknowledgements

892 | Photochem. Photobiol. Sci., 2013, **12**, 883–894

This journal is © The Royal Society of Chemistry and Owner Societies 2013

Notes and references

1 J. Desilvestro, M. Gratzel, L. Kavan, J. Moser and J. Augustynski, *J. Am. Chem. Soc.*, 1985, **107**, 2988.

2 M. K. Nazeeruddin, P. Liska, J. Moser, N. Vlachopoulos and M. Gratzel, *Helv. Chim. Acta*, 1990, **73**, 1788.

3 Other names for this technology are dye-sensitized nanostructured solar cells, mesoscopic injection solar cells, nanosolar cells, artificial leaves, or Gratzel cells. In this paper, we use the acronym DSSCs for dye-sensitized solar cells.

4 B. O'Regan and M. Gratzel, *Nature*, 1991, **353**, 737.

5 M. K. Nazeeruddin, A. Kay, I. Rodicio, R. Humphry-Baker, E. Mueller, P. Liska, N. Vlachopoulos and M. Gratzel, *J. Am. Chem. Soc.*, 1993, **115**, 6382.

6 M. K. Nazeeruddin, F. De Angelis, S. Fantacci, A. Selloni, G. Viscardi, P. Liska, S. Ito, B. Takeru and M. Grätzel, *J. Am. Chem. Soc.*, 2005, **127**, 16835.

7 A. Yella, H.-W. Lee, H. N. Tsao, C. Yi, A. K. Chandiran, Md. K. Nazeeruddin, E. W.-G. Diau, C.-Y. Yeh, S. M. Zakeeruddin and M. Grätzel, *Science*, 2011, **334**, 629.

8 M. K. Nazeeruddin, P. Pechy, P. Liska, T. Renouard, S. M. Zakeeruddin, R. Humphry-Baker, P. Comte, L. Cevey, E. Costa, V. Shklover, L. Spiccia, G. B. Deacon, C. A. Bignozzi and M. Gratzel, *J. Am. Chem. Soc.*, 2001, **123**, 1613.

9 M. Gratzel, *Inorg. Chem.*, 2005, **44**, 6841–6851.

10 G. Giuffrida, G. Calogero, G. Guglielmo, V. Ricevuto, M. Ciano and S. Campagna, *Inorg. Chem.*, 1993, **32**, 1179–1183.

11 G. Calogero, G. Giuffrida, S. Serroni, V. Ricevuto and S. Campagna, *Inorg. Chem.*, 1995, **34**, 541–545.

12 G. Giuffrida, G. Calogero, V. Ricevuto and S. Campagna, *Inorg. Chem.*, 1995, **34**, 1957–1960.

13 R. Argazzi, N. Y. Murakami Iha, H. Zabri, F. Odobel and C. A. Bignozzi, *Coord. Chem. Rev.*, 2004, **248**, 1299–1316.

14 A. Hagfeldt, G. Boschloo, L. Sun, L. Kloo and H. Pettersson, *Chem. Rev.*, 2010, **110**, 6595–6663.

15 G. Calogero, G. Di Marco, S. Caramori, S. Cazzanti, R. Argazzi and C. A. Bignozzi, *Energy Environ. Sci.*, 2009, **2**, 1162.

16 G. Calogero, J.-H. Yum, A. Sinopoli, G. Di Marco, M. Gratzel and M. K. Nazeeruddin, *Sol. Energy*, 2012, **86**(5), 1563.

17 X. F. Wang, C. H. Zhan, T. Maoka, Y. Wada and Y. Koyama, *Chem. Phys. Lett.*, 2007, **447**, 79.

18 G. Calogero and G. Di Marco, *Sol. Energy Mater. Sol. Cells*, 2008, **92**, 1341.

19 G. Calogero, G. Di Marco, S. Cazzanti, S. Caramori, R. Argazzi, A. Di Carlo and C. A. Bignozzi, *Int. J. Mol. Sci.*, 2010, **11**, 254.

20 G. Calogero and G. Di Marco, Photoelectrochemical solar cell comprising sensitizing anthocyanin and betalain dyes of vegetal or synthetic origin, or mixtures thereof, WO/2010/044122, 2010.

21 R. Brouillard and Chemical structure of anthocyanins, in *Anthocyanins as Food Color*, ed. P. Markakis, Academic Press, New York, 1982, pp. 1–40.

22 L. Carbita, T. Fossen and O. M. Andersen, Colour and stability of six common anthocyanin 3-glucosides in aqueous solutions, *Food Chem.*, 2000, **68**, 101–107.

23 G. A. Cooper-Driver, Contributions of Jeffrey Harborne and co-workers to the study of anthocyanins, *Phytochemistry*, 2001, **56**, 229–236.

24 A. Bakowska-Barczak, *Pol. J. Food Nutr. Sci.*, 2005, **14/55**, 107–116.

25 *Flavonoids. Chemistry, Biochemistry and Application*, ed. Ø. M. Anderson and K. R. Markham, Taylor & Francis Group, CRC Press, NY, 2006.

26 E. Haslam, *Practical Polyphenols. From Structure to Molecular Recognition and Physiological Action*, Cambridge University Press, Cambridge, 1998.

27 J. B. Harbone, *The Flavonoids—Advances in Research since 1980*, Chapman & Hall, London, 1988.

28 J. B. Harbone and C. A. Williams, *Nat. Prod. Rep.*, 2001, **18**, 310–333.

29 C. A. Williams and R. J. Grayer, *Nat. Prod. Rep.*, 2004, **21**, 539–573.

30 C. V. Nigel and R. J. Grayer, *Nat. Prod. Rep.*, 2008, **25**, 555–611.

31 K. Yoshida, M. Mori and T. Kondo, *Nat. Prod. Rep.*, 2009, **26**, 884–915.

32 T. Goto and T. Kondo, *Angew. Chem., Int. Ed. Engl.*, 1991, **30**, 17–33.

33 K. Yoshida, T. Kondo, Y. Okazaki and K. Katou, *Nature*, 1995, **373**, 291.

34 M. J. Melo, M. Moncada and F. Pina, *Tetrahedron Lett.*, 2000, **41**, 1987–1999.

35 V. Freitas and N. Mateus, *Anal. Bioanal. Chem.*, 2010, **401**, 1467.

36 F. Pina, M. Maestri and V. Balzani, *Chem. Commun.*, 1999, 107–114.

37 F. Pina, M. Maestri and V. Balzani, *Supramolecular Chemistry, in Handbook of Photochemistry and Photobiology*, ed. H. S. Nalwa, ASP, 2003, vol. 3, ch. 9.

38 F. Pina, M. Maestri and V. Balzani, in *Molecular Switches*, ed. B. L. Feringa, Wiley-VCH, 2001, ch. 10.

39 F. Pina, M. J. Melo, C. A. T. Laia, A. Jorge Parola and J. C. Lima, *Chem. Soc. Rev.*, 2012, **41**, 869.

40 A. G. Perkin and A. E. Everest, The Natural Organic Coloring Matters, Longmans, Green and Co., 1918, facsimile 2011, Nabu, Public Domain Reprints.

41 *Flavonoids. Chemistry, Biochemistry and Application*, ed. Ø. M. Anderson and K. R. Markham, Taylor & Francis Group, CRC Press, NY, 2006.

42 R. Robinson, Nobel Lecture, 1947, available at http://www.nobelprize.org/

43 R. Willstatter, Nobel Lecture, 1915, available at http://www.nobelprize.org/

44 F. M. Dean, *Naturally Occurring Oxygen Ring Compounds*, Butterworths, London, 1963, ch. 13, pp. 388–484.

45 F. W. Küster and A. Thiel, *Tabelle per le Analisi Chimiche e Chimico-Fisiche*, Hoepli, Milano, 12th edn, 1982, pp. 157–160.

46 F. Pina, A. Roque, M. J. Melo, M. Maestri, L. Belladelli and V. Balzani, *Chem.–Eur. J.*, 1998, **4**, 1184–1191.

47 T. Malkin and M. Nierenstein, *J. Am. Chem. Soc.*, 1931, **53**, 239–242.

48 R. Robinson and D. D. Pratt, *J. Chem. Soc.*, 1922, 1577–1585.

49 M. C. Moncada, S. Moura, M. J. Melo, A. Roque, C. Lodeiro and F. Pina, *Inorg. Chim. Acta*, 2003, **356**, 51–61.

50 C. Lee, W. Yang and R. G. Parr, *Phys. Rev. B*, 1988, **37**, 785–789.

51 A. D. Becke, *J. Chem. Phys.*, 1993, **98**, 5648–5652.

52 L. Estévez and R. A. Mosquera, *J. Phys. Chem. A*, 2007, **111**, 11100–11109.

53 A. Amat, C. Clementi, F. De Angelis, A. Sgamellotti and S. Fantacci, *J. Phys. Chem. A*, 2009, **113**(52), 15118–15126.

54 G. Calogero, P. Calandra, A. Irrera, A. Sinopoli, I. Citro and G. Di Marco, *Energy Environ. Sci.*, 2011, **4**, 1838.

55 A. R. Katritzky, P. Czerney, J. R. Levell and W. Du, *Eur. J. Org. Chem.*, 1998, 2623–2629.

56 T. Mas, *Synthesis*, 2003, 1878–1880.

57 A. Calzolari, D. Varsano, A. Ruini, A. Catellani, R. Tel-Vered, H. B. Yildiz, O. Ovits and I. Willner, *J. Phys. Chem. A*, 2009, **113**, 8801–8810.

58 N. J. Cherepy, G. P. Smestad, M. Grätzel and J. Z. Zhang, *J. Phys. Chem. B*, 1997, **101**, 9342.

59 M. C. Moncada, D. Fernández, J. C. Lima, A. J. Parola, C. Lodeiro, F. Folgosa, M. J. Melo and F. Pina, *Org. Biomol. Chem.*, 2004, **2**, 2802–2808.